

# Computational Model of Adsorption for Hydroxybenzoate Saxitoxin Derivatives (GCs) on Graphene Surface <sup>†</sup>

Mercedes Álvarez <sup>1,\*</sup>, Manuel Lolo <sup>2</sup> and Álvaro Antelo <sup>1,\*</sup> <sup>1</sup> Laboratorio CIFGA S.A., Avenida Benigno Rivera, No. 56, 27003 Lugo, Spain<sup>2</sup> AMSLAB, Avenida Benigno Rivera, No. 56, 27003 Lugo, Spain; manuel.lolo@ams-lab.com

\* Correspondence: mercedes.alvarez@cifga.com (M.Á.); alvaro.antelo@cifga.com (Á.A.)

<sup>†</sup> Presented at the 27th International Electronic Conference on Synthetic Organic Chemistry (ECSOC-27), 15–30 November 2023; Available online: <https://ecsoc-27.sciforum.net/>.

**Abstract:** Here, we report on the determination of the supramolecular adsorption of hydroxybenzoate derivatives (GC toxins) of saxitoxin to a pristine graphene surface using the computational method, MMFF94 Force Field implemented in the Chem Office package. We use a simple model with the GC molecule centred on the graphene surface, to simulate the interaction of GC molecule stacking on the graphene system, avoiding edge interactions. We find that the formation of the GC–graphene complex is favourable for all GC molecules. The results of our model are in good agreement with chromatographic elution results on the graphite surface, specifically the Hypercarb column. We predict that these aromatic saxitoxin derivatives possess a higher adsorption energy than non-aromatic ones.  $\pi$ - $\pi$  stacking can be regarded as being a prevalent contribution compared to non-aromatic analogues. Furthermore, MMFF94 adsorption results yield qualitative agreement with experiments within N-OH and N-H sub-families: in the computational model, the interaction energy value's order is GC6-GC5-GC4-GC3-GC2-GC1 (the highest adsorption energy). In the experimental Hypercarb model, the elution order is GC3-GC6-GC2-GC5-GC4-GC1 (the highest retention time). The proposed MMFF94 research framework works well in the assessment of chromatographic selectivity. This simple model has the potential for use in predicting the qualitative interactions of small polar molecules and graphene, which sheds light on the application of computational techniques to help in analytical method development.

**Keywords:** MMFF94; graphene; supramolecular; saxitoxin; paralytic shellfish poisoning; Hypercarb



**Citation:** Álvarez, M.; Lolo, M.; Antelo, Á. Computational Model of Adsorption for Hydroxybenzoate Saxitoxin Derivatives (GCs) on Graphene Surface. *Chem. Proc.* **2023**, *14*, 94. <https://doi.org/10.3390/ecsoc-27-16038>

Academic Editor: Julio A. Seijas

Published: 15 November 2023



**Copyright:** © 2023 by the authors. Licensee MDPI, Basel, Switzerland. This article is an open access article distributed under the terms and conditions of the Creative Commons Attribution (CC BY) license (<https://creativecommons.org/licenses/by/4.0/>).

## 1. Introduction

In this manuscript, we study the adsorption of natural hydroxybenzoate derivatives of saxitoxin on graphene, calculated using the MMFF94 force field. Our choice of GC–graphene systems is motivated by two key reasons:

- (i) It is computationally feasible to calculate free energies of adsorption of GC–graphene systems.
- (ii) Saxitoxin derivatives are one of the most relevant groups of toxins.

Saxitoxin (STX) and its analogues are responsible for paralytic shellfish poisoning, and the group of toxins that make up this group are called PSP toxins. Chemically, PSP toxins possess 3,4-propinoperhydropurine tricyclic, a backbone common to all analogues in this group, but differing in the combinations of hydroxyls and sulfates primarily at four positions of the molecule, R1–R4 (Figure 1). STX belongs to the large family of guanidine-containing marine natural products, particularly two guanidine groups, which are responsible for its high hydrophilicity and polarity. The guanidine groups are associated with two proton dissociations at pKa 8.1–8.4 and 11.3–11.6, which are assigned to the guanidinium moieties centred at C8 (imidazole guanidine) and C2 (pyrimidine guanidine), respectively [1].

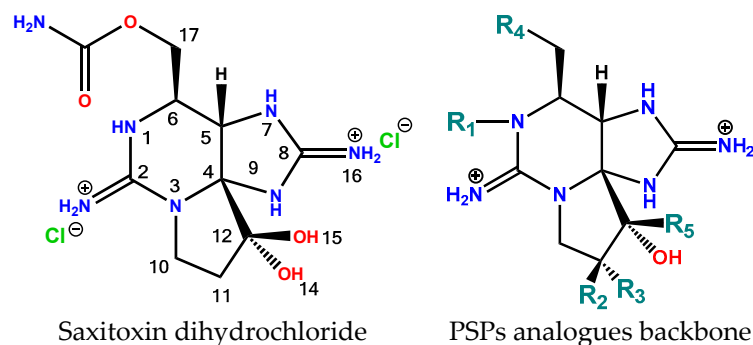


**Figure 1.** Saxitoxin and the structural backbone of PSPs family. Highly polar bis-guanidinium small molecule. Laboratorio CIFGA [2] has various standards and certified reference materials for PSPs but is also in the process of developing new ones, such as: doSTX, GC1&2, GC3, GC4&5, GC6, dcGTX1&4, 12- $\beta$ -deoxySTX, M1, and M3.

In addition to the strong influence of pH on the structure and stability of saxitoxins, temperature also has a significant influence on their stability. Overall, saxitoxin and derivatives are stable in weakly acidic solutions but decompose quickly in alkaline media, depending on the structure of the analogue. The stability of PSP toxins decreases dramatically with temperature, especially at temperatures above room temperature. At higher temperatures ( $>50\text{ }^{\circ}\text{C}$ ), the stability of each analogue drops dramatically to hours or even a few minutes.

High temperatures combined with high pH values lead to greater instability and faster breakdown of toxins. It is important to keep in mind that pH and temperature variations lead to conversions between different analogues and in new metabolites of paralytic shellfish toxins [3]. Changing pH and temperature could be considered to achieve the next objectives:

- (i) Maximization of the average final product, and
- (ii) Minimization of the degradation product concentration.

For example, C3&4 is more thermolabile than GTX1&4, with approximately five times higher degradation rates, even at lower pH values. See Figure 2 for kinetics data. The conversion of C3&4 into dcGTX1&4 is more effective than GTX1&4. Qualitative analysis of the kinetics of GTX1&4 and NEO hydrolysis signals shows that dcGTX1&4 and dcNEO are labile to conventional hydrolysis conditions, and are therefore transient intermediates, although final degradation products were not detected by the MS/MS used in this study of Laboratorio CIFGA.

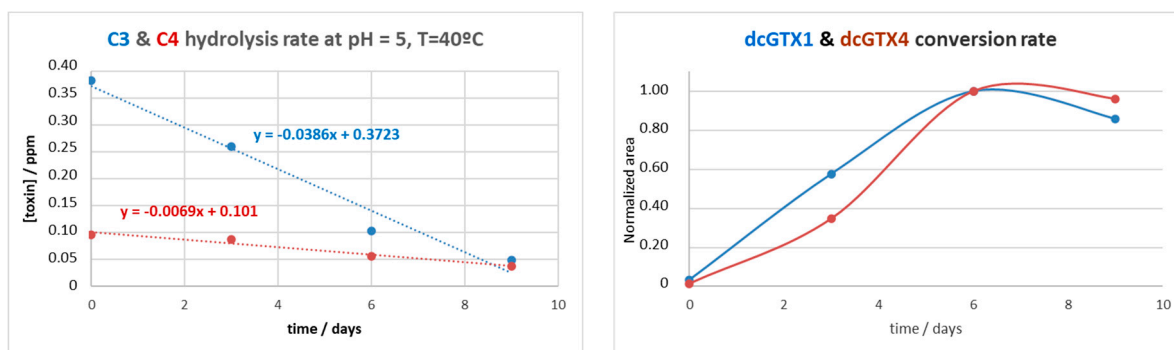


**Figure 2.** Cont.

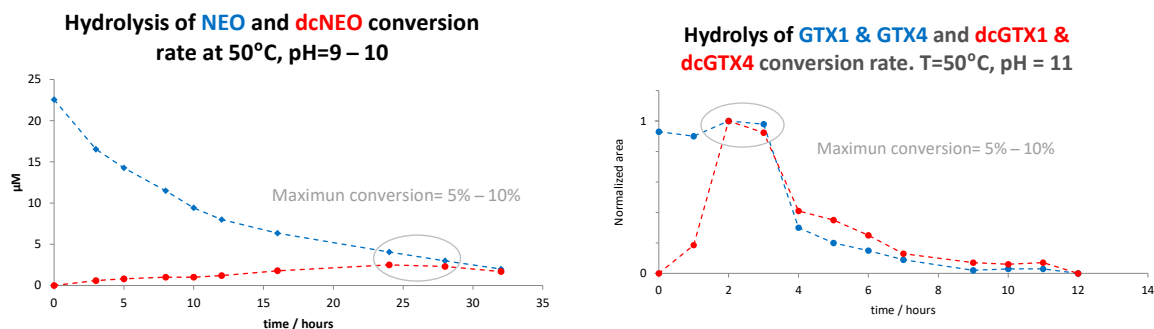


**Figure 2.** Laboratorio CIFGA S.A. internal data for some kinetics of PSPs hydrolysis at different pH and temperature. In the narrow region of time evaluated, the results indicate that C3&C4 hydrolysis follows zero-order under Curtin–Hammett control kinetics, whereas NEO and GTX1&4 hydrolysis reactions exhibit apparent first-order kinetic. The low recovery of dcNEO and dcGTX1&4 reveals that other collateral reactions are more efficient in the initial PSP degradation. The time-course of dcGTX1&4 formation depicts an unknown degradation in the same way as GTX1&4.

Among the more than 50 known analogues, the group with an aromatic substituent at position R4 is called GC analogues, which comprises three sub-groups according to aromatic substituent [4]:

- p-hydroxybenzoate: GC1 to GC6 (Figure 3)
- o,m-dihydroxybenzoate: GC1a to GC6a
- p-sulfobenzoate: GC1b to GC1b

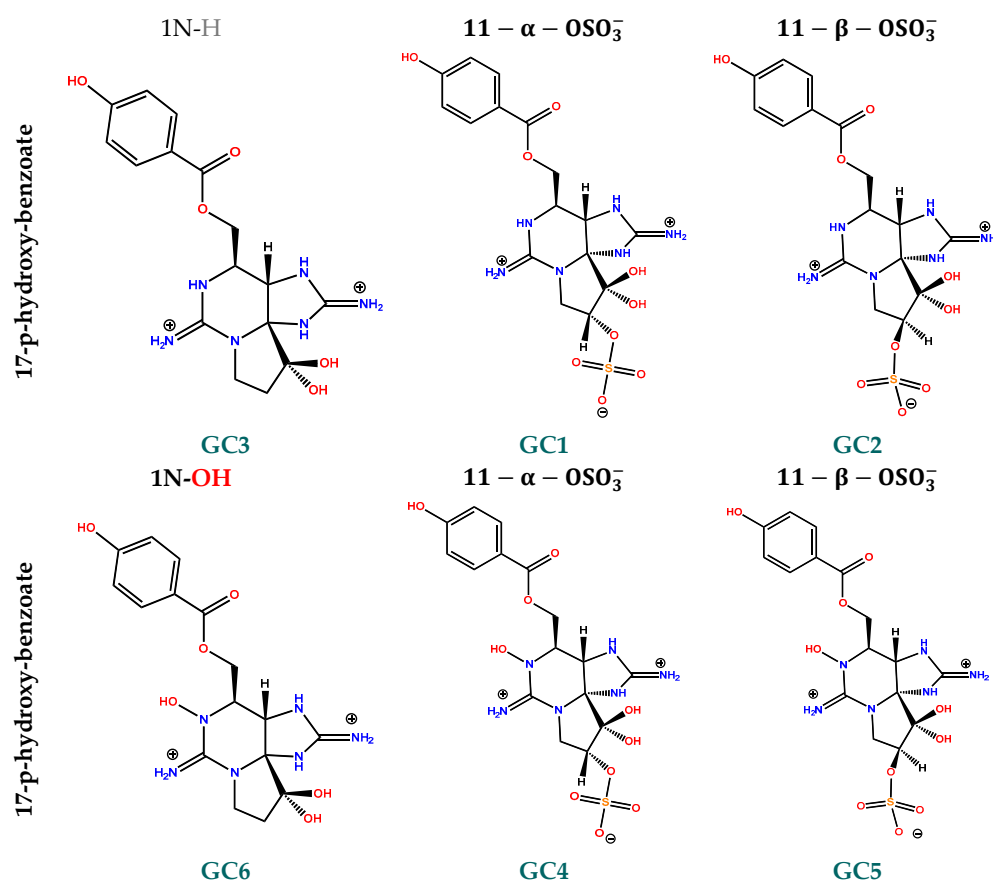


**Figure 3.** 2D structure of p-hydroxybenzoate (GC1 to GC6) PSPs derivatives. Hydroxybenzoate saxitoxins are a group of toxins produced by *G. catenatum* strains that belong to the larger group of paralytic shellfish toxins.

The toxicity of these analogues is not yet precisely known, but they have been identified in strains of *G. catenatum* isolated in Portugal, Spain, China, Japan, and Uruguay, thus demonstrating their worldwide distribution [5]. These PSPs are retained over C18 bulk and are therefore also referred to as hydrophobic PSP.

Like PSP analogues, GC toxins are unstable in alkaline media. The hydrolysis of benzoate analogues progresses rapidly with increasing amounts of base, but the decarbamoyl gonyautoxin-type hydrolysis products were short-lived and transformed into decarbamoyl saxitoxin-type analogues [6].

The GC hydrolysis profile is quite similar to that of gonyautoxins. The profile is biphasic and characterized by an initial increase in the rate of decarbamoyl formation through a preliminary first-order kinetic profile and a final stage in which decarbamoyl degradation occurs. Lowering the test temperature from 50 °C to 4 °C reduces the reaction rate of hydrolysis, the rate of degradation side reactions, and although the conversion is better, it is still low (5–10%).

Data analysis shows that the hydrolysis kinetics are sensitive to R4 substituent. The qualitative kinetic order found is  $C3\&4 \gg GC4\&5 > GTX1\&4$  and  $GTX6 \gg GC6 > NEO$ , while the qualitative conversion product recovery is  $C3\&4 \gg GC4\&5 \geq GTX1\&4$  and  $GTX6 \gg GC6 \geq NEO$ . It is important to note that the rate of a reaction can be affected by various factors such as temperature, concentration, and the presence of a catalyst.

Conventional carbon filtration media are often used to remove water pollutants in water treatment. Carbon materials possess unique sorption properties. Carbon-based adsorbents exhibit the property of adsorbing interaction with highly polar, ionic, or ionizable organic or inorganic compounds [7]. Among the different types of carbon frameworks, we focus on the following: Porous graphitic carbon (PGC) and graphene. In this study, we compared the experimental results of the PGC framework with the computational adsorption over graphene.

The porous graphitic carbon structure was entirely composed of stacks of graphitic sheets and remained stable at high pH and temperature levels. The surface of PGC is characterized by a cloud of delocalized electrons. Therefore, as polar analytes approach the surface, an induced dipole is created as the electrons drop toward or away from the polar analyte, allowing the analyte to be retained. This electrostatic effect was described by Ross and Knox as the polar retention effect on graphite (PREG) [8]. PGC exhibits high selective adsorption ability in separating polar uncharged species, highly polar compounds with different spatial molecular structures (including structural isomers), and ionic/charged species via high-performance liquid chromatography (HPLC). C8 or C18 reverse phases are often less effective or even fail to retain this class of compounds [9]. PGC exhibits high column efficiency for polar compounds and improved retention of compounds that typically require hydrophilic interaction liquid chromatography (HILIC) for retention. The ability to retain and separate polar and hydrophilic molecules can be a major challenge in method development [10].

Graphene (Figure 4) is a now well-known single layer of carbon arranged in a two-dimensional honeycomb lattice with a strong  $\sigma$  bond, and the  $\pi$  electrons on graphene can move more freely than those on graphite. Different graphene-based adsorbents have been found to have diverse adsorption capacities against different pollutants [11].

MMFF94 [12] energies and geometries were used to evaluate the trend for intermolecular interaction energies and geometries in the supramolecular study between graphene and adsorbates. The prediction of elution order in high-performance liquid chromatography (HPLC) could be useful in developing analytical methods and for analyte identification. Force fields have the advantage over ab initio methods in that they require significantly less computational effort. However, their accuracies are substantially more limited than those of more advanced ab initio electronic structure methods [13].

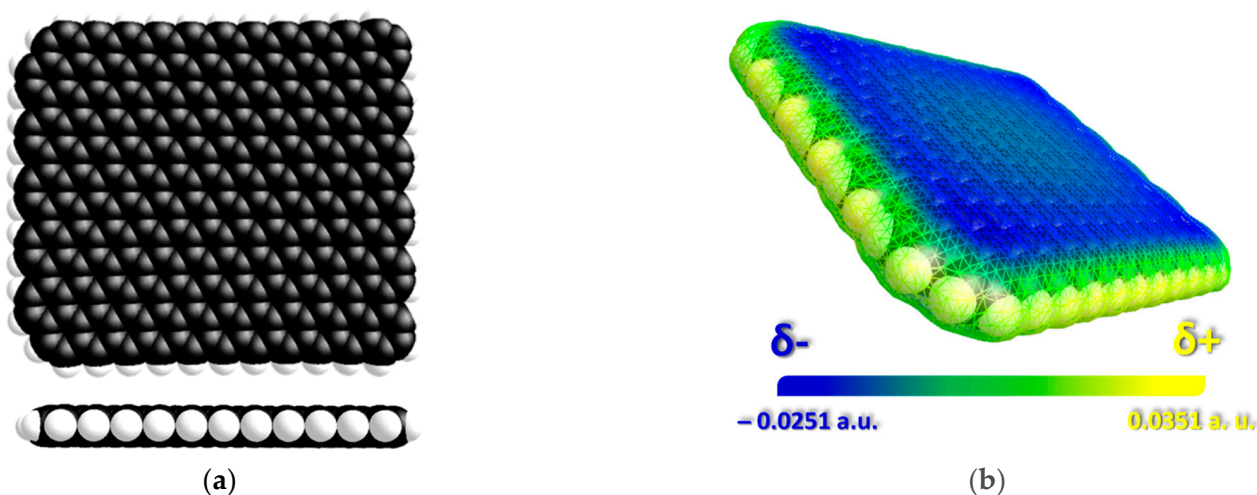


**Figure 4.** MMFF94 Minimized Chemical 3D frameworks pristine graphene sheet (286 carbon atoms,  $C_{286}H_{46}$ ) used in this work (a) and Molecular Electrostatic Potential map (MEP) surface for graphene as generated by VEGA ZZ 3.0.0 [14] (b). We can find that the C atoms in the graphene sheet have the most significant electron density values (blue), so they can act as acceptors for electrophilic molecules. In contrast, the edges have less (yellow), so nucleophilic units are more readily accepted.

Keep in mind that the approach chosen to predict supramolecular interactions depends on the particular systems studied, the goals of the research, and the resources available. Additionally, whenever possible, it is a good idea to validate computational predictions with experimental results. Supramolecular interactions often include non-covalent interactions, such as hydrogen bonds, van der Waals interactions, electrostatic interactions, and  $\pi$ - $\pi$  stacking. These interactions can be complex and require a detailed representation to accurately predict their behavior.

We have previously reported experimental and computational studies on the association of water-soluble saxitoxin and tetrodotoxin analogues with pristine graphene and graphene oxide [15,16]. An applicable retention time prediction model must not only be predictive but also be able to predict analytes in the correct order. This becomes even more obvious in very complex mixtures with hundreds of compounds (such as peptides in a proteomic mixture) [17].

## 2. Methods

Molecular modelling was performed using the Merck Molecular Force Field 94 (MMFF94) implemented in Chem3D version 18.1 software from CambridgeSoft [18].

As in our previous works, the procedure involves the following steps:

1. The 2D structures of all compounds were created in the builder module of ChemDraw software. The 2D structures of the compounds were then transferred to Chem3D.
2. Conformations were optimised using Merck Molecular Force Field 94 (MMFF94). Geometry optimizations for all molecules were calculated using root mean square convergence criteria for the potential energy surface gradient of 0.001 kcal/mol.  $E_{toxin}$  is the potential energy of the toxin (adsorbate), and  $E_{graphene}$  is the potential energy of graphene (substrate).

The MMFF94 force field, like many other force fields in molecular mechanics, depends on the initial conformation of the molecules under study. Different starting geometries for GC toxins were tested because no minimum energy geometry can lead to unrealistic results. The different initial conformations led to a change in the spatial distribution of the hydroxybenzoate group and the arrangement of intermolecular hydrogen bonds.

After energy minimization, a visual inspection of the optimised geometry is performed to verify that there are no chemical inconsistencies.

3. A bottom-up scheme was employed where the starting topology consists of a toxin randomly positioned in the middle of the pristine graphene layer (286 carbon atoms, C<sub>286</sub>H<sub>46</sub>) with a distance of 4 Å to 7 Å. Subsequently, the energy and geometry of the supramolecular complex were optimised without fixing the position of the graphene atoms in space to obtain  $E_{supramolecular}$  (potential energy of the complex in vacuum at the local minimum).
4. To achieve a comprehensive understanding, we computed the adsorption of 6 hydroxybenzoate (GC) and 2 non-aromatic derivatives of STX on graphene using the MMFF94 force field.
5. Calculations were performed on an Intel Dual Core 2.6 GHz computer with 8 GB RAM. Force fields are particularly suitable for conformational searches due to their very low computational cost.
6. The simulation parameters were chosen as follows:
  - 6.1 Minimizations were performed without solvents (vacuum is the medium of minimizations). The supramolecular stoichiometry of these complexes is 1:1.
  - 6.2 The final supramolecular complex is a local minimum energy. To obtain a value for statistical energy proposal, several computational energy approaches are considered. 0.34 kcal/mol was the maximum difference between the minimum planar conformational energy of pristine graphene and the computed energy of the layer after supramolecular interaction. In addition, further uncertainty may arise due to the proximity of the molecule to the hydrogen-terminated edges. An uncertainty of 0.4 kcal/mol is considered an average value for a proximity of 5 Å to 8 Å of the nearest atom to terminal hydrogen. Therefore, 0.74 kcal/mol is used as the minimum adsorption energy difference to assess qualitative differences.
  - 6.3 Final supramolecular structures with distances less than 5 Å from boundaries were not considered.
  - 6.4 Saxitoxin derivatives possess two guanidinium groups because they exist in cationic form at lower pH values. In this research, we only evaluate the interaction with this form. For simplicity, a new approach is used where the guanidinium group with the charge in the (C = N<sub>2</sub><sup>+</sup>) group is examined instead of evaluating the three resonance forms. In addition, in the presence of a sulfated group on C11, a negative charge is implemented.
  - 6.5 The topology of the initial toxin alignment is critical to the value of this method. The GC molecules were centred over the graphene layer so that hydrogen bonds that held the molecules to the edge of the model phase were not possible. The GC interaction with graphene is evaluated by comparing three different approaches: both guanidinium groups aligned to graphene, one guanidinium group N7-C8-N9, and one as the base of the guanidinium N1-C2-N3 group, Figure 5.
  - 6.6 The binding energy of individual toxins adsorbed on pristine graphene was determined by subtracting the energy of the toxin and the graphene model from that of the supramolecular complex.

$$\Delta E = E_{supramolecular} - (E_{toxin} + E_{graphene})$$

where  $E_{supramolecular}$  is the potential energy of the complex in vacuum at the minimum, and  $E_{toxin}$  and  $E_{graphene}$  are the potential energies of the adsorbate and substrate, which are separated by an infinite distance.

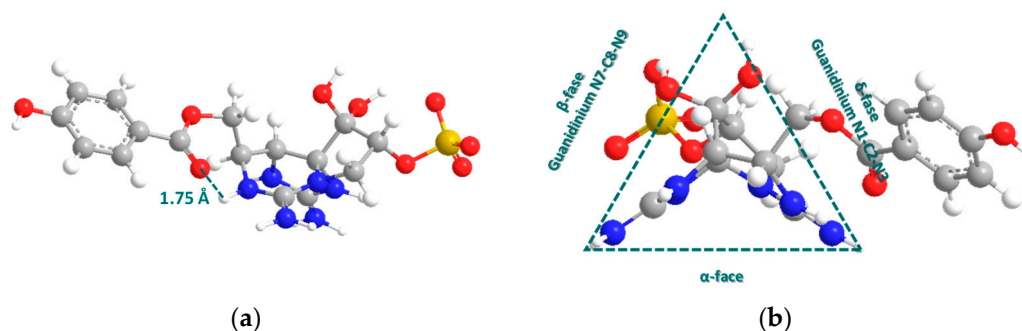


**Figure 5.** (a) Distance of tentative intramolecular hydrogen bonding in GC1. (b) Stereo-structure of GC1 with our triangular side nomenclature to define three-dimensional interaction with graphene. These tests are useful to differentiate two local minimum conformers since the initial geometry of the GC molecule can have a significant impact on the calculated energies and structure of the supramolecular complex.

### 3. Results and Discussion

The most stable MMFF94 geometry for GC molecules and pristine graphene were used as a reference structure to better understand the interaction mode between the two molecules. Optimised structures of saxitoxin derivatives are shown in Figure 6. The most important conformational change in the structure of GCs was found in the spatial arrangement of the hydroxybenzoate group. The lowest energy conformation with unfolded hydroxybenzoate is shown in the left-side column. The energy difference between the two optimised structures is about 2–3 kcal/mol for GC1 and GC2, instead of <0.2 kcal/mol for GC4 and GC5. For GC5, only the minimum energy of folded hydroxybenzoate is found, but a difference of <0.2 kcal/mol between the two structures. Interactions with folded hydroxybenzoate do not result in good interaction energies with graphene; most minimizations result in the unfolding of the hydroxybenzoate in the final structure.

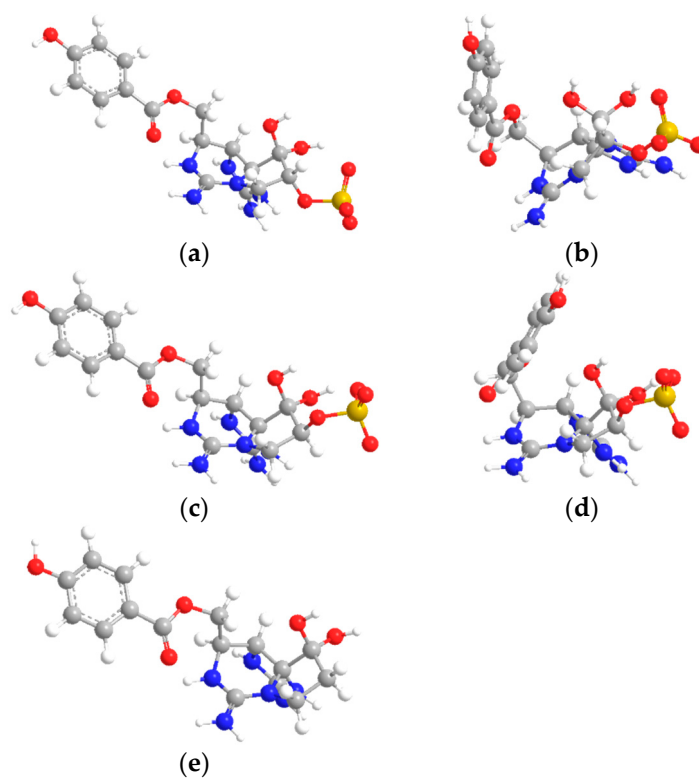


**Figure 6.** *Cont.*

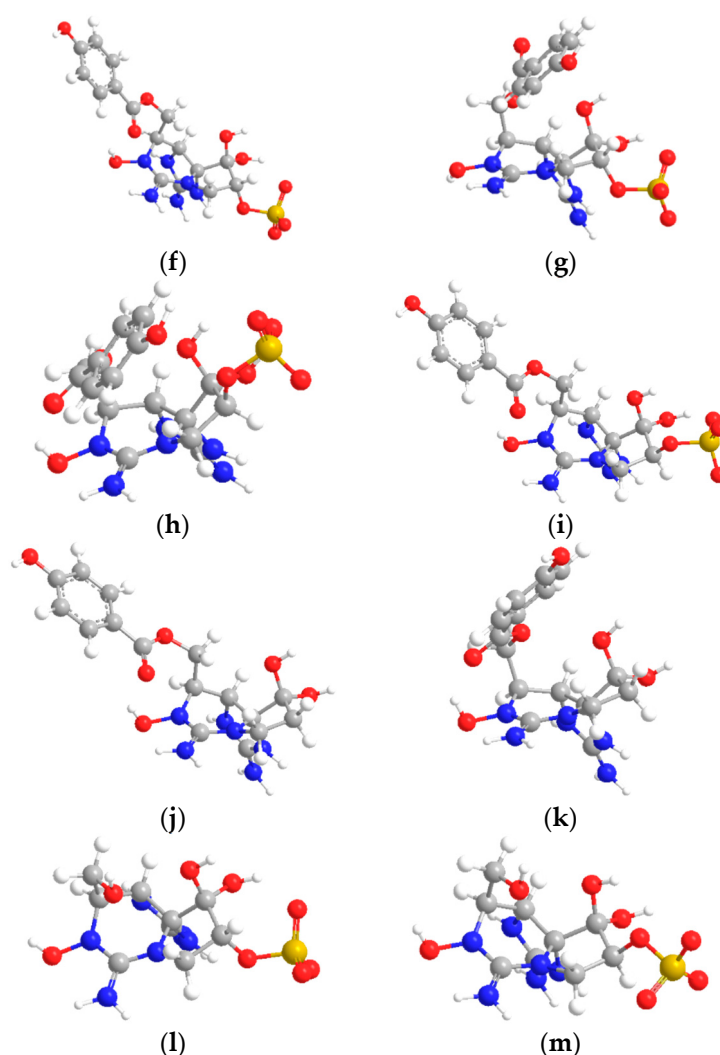


**Figure 6.** Minimum optimised geometry for saxitoxin derivatives: (a) GC1 with unfolded hydroxybenzoate, (b) GC1 folded, (c) GC2 unfolded, (d) GC2 folded, (e) GC3, (f) GC4 unfolded, (g) GC4 folded, (h) GC5 folded, (i) GC5 unfolded, (j) GC6 unfolded, (k) GC6 folded, (l) dcGTX1, (m) dcGTX4. The left side part unveils hydroxybenzoate's lowest minimum 3D structure.

The adsorption of GC toxins over graphene was evaluated without counter-anions, considering only the guanidinium-cationic ( $C = N_2^+$ ) and  $SO_3^-$  arrangements. The corresponding energy values are listed in Table 1. When GC molecules are adsorbed on the graphene, GC gradually approaches the surface, and the graphene surface is slightly deformed (curved) as a result of the adsorption of GC. After about 10,000–16,000 steps, a local equilibrium structure is achieved. To incorporate graphene curvature deformation into the nonbonding interactions, we used the adaptive difference of 0.35 kcal/mol to predict the relative retention order.

**Table 1.** Energy values of CGs, pristine graphene, and supramolecular complexes.

Molecule	Supramolecular Approach	$E_{molecule}/\text{kcal}\cdot\text{mol}^{-1}$	$\Delta E/\text{kcal}\cdot\text{mol}^{-1}$
Graphene	-	1491.71	
GC1	$\alpha$ -face		-48.14
	$\beta$ -face	-222.97	-37.54
	$\delta$ -face		-40.12

Table 1. Cont.

Molecule	Supramolecular Approach	$E_{molecule}/\text{kcal}\cdot\text{mol}^{-1}$	$\Delta E/\text{kcal}\cdot\text{mol}^{-1}$
GC2	$\alpha$ -face	−221.42	−43.53
	$\beta$ -face		−38.39
	$\delta$ -face		−41.59
GC3	$\alpha$ -face	−202.73	−42.71
	$\beta$ -face		−34.38
	$\delta$ -face		−37.87
GC4	$\alpha$ -face	−137.55	−39.57
	$\beta$ -face		−37.42
	$\delta$ -face		−40.60
GC5	$\alpha$ -face	−136.04	−35.01
	$\beta$ -face		−37.84
	$\delta$ -face		−38.63
GC6	$\alpha$ -face	−117.74	−34.17
	$\beta$ -face		−36.83
	$\delta$ -face		−37.11
dcGTX1	$\alpha$ -face	−148.46	−33.09
	$\beta$ -face		−32.05
	$\delta$ -face		−28.79
dcGTX4	$\alpha$ -face	−144.73	−30.18
	$\beta$ -face		−35.25
	$\delta$ -face		−28.66

Two approaching stages were visually inspected before a local minimum equilibrium structure was reached. For all molecules considered in this study, the weak adsorption of GC on a pristine graphene sheet disrupts the intramolecular geometry of both molecules. For distances  $>4$  Å, the trajectory approach shows that the (attractive) interaction is dispersive. In the first stage, the noncovalent ion- $\pi$  and XH- $\pi$  stackings are responsible for the initial supramolecular complex between GC and graphene. In the second stage, the stabilization can be associated with the presence of  $\pi$ - $\pi$  stacking interactions.

Experimental and molecular calculations show that the GC1 molecule has the highest retention time and absorption energy, respectively. The configuration optimised for GC1 shows an almost extended coplanar arrangement with a graphene layer with sulfate groups near the  $\pi$  surface (Figure 7).

Hydroxybenzoate/graphene angles are also examined. The 3D model of the GC1 minimal structure shows a quasi-planar interaction between guanidinium and sulfate group with the graphene layer. The angle between the hydroxybenzoate and graphene plane is  $4.59^\circ$ , while an average plane of van der Waals contact atoms of guanidinium has an angle  $< 1^\circ$  with the graphene plane.

The hydroxybenzoate centroid is located at 3.358 Å above the graphene mean plane. Note that the contact of guanidinium with the surface is closer, approximately (2.5–3.0 Å) than that of sulfate groups (3.2–3.4 Å).

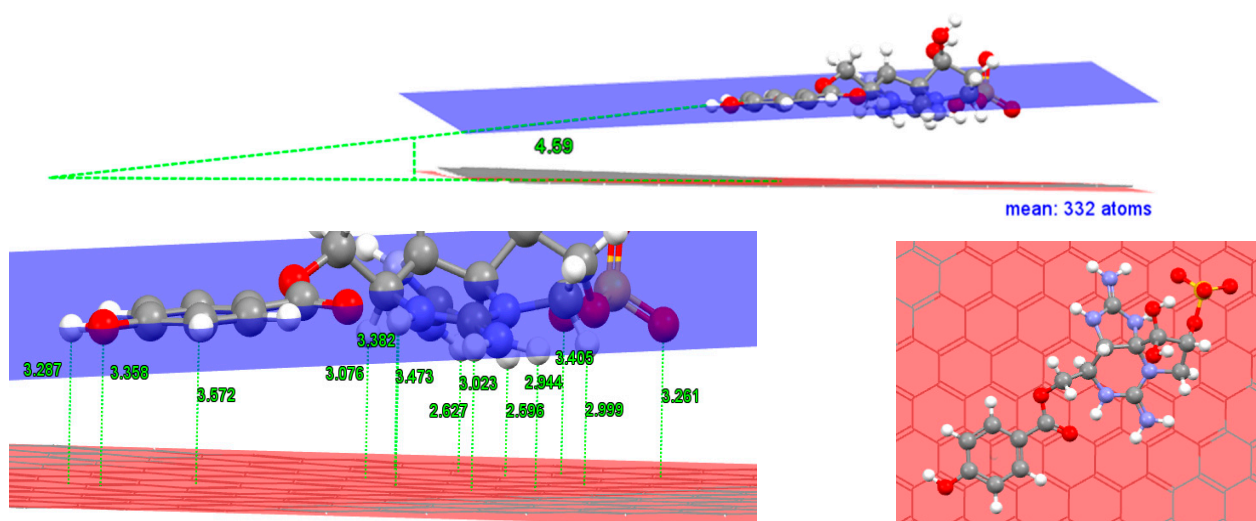


**Figure 7.** Distances were calculated using Mercury 3.8 [19] software for GC1's lowest energy supramolecular complex. The red plane is the mean of all atoms of graphene. The blue plane is the mean of six carbons of hydroxybenzoate moiety. The centroid from these 6 carbons is located at 3.572 Å.

The non-aromatic fragment of the GC1 molecule presents 10 close contacts below the hydroxybenzoate plane. The top view of this interaction shows that mainly ion- $\pi$  interaction occurs when the cation and anion are centred directly over the  $\pi$ -system and are in direct van der Waals contact. In addition, hydroxybenzoate is slipped from each benzene group of graphene.

GC1 adsorbs significantly stronger than GC2. GC1 has a longer retention time and theoretically a lower energy complex. GC2 presents 8 close contacts, and the sulfate group is located on the other side of the hydroxybenzoate plane and therefore results in less anion- $\pi$  interaction (Figure 8). In both epimer pairs, GC1 vs. GC2 and GC4 vs. GC5, the sulfate group in the 11- $\beta$  position leads to a result with lower absorption energy.

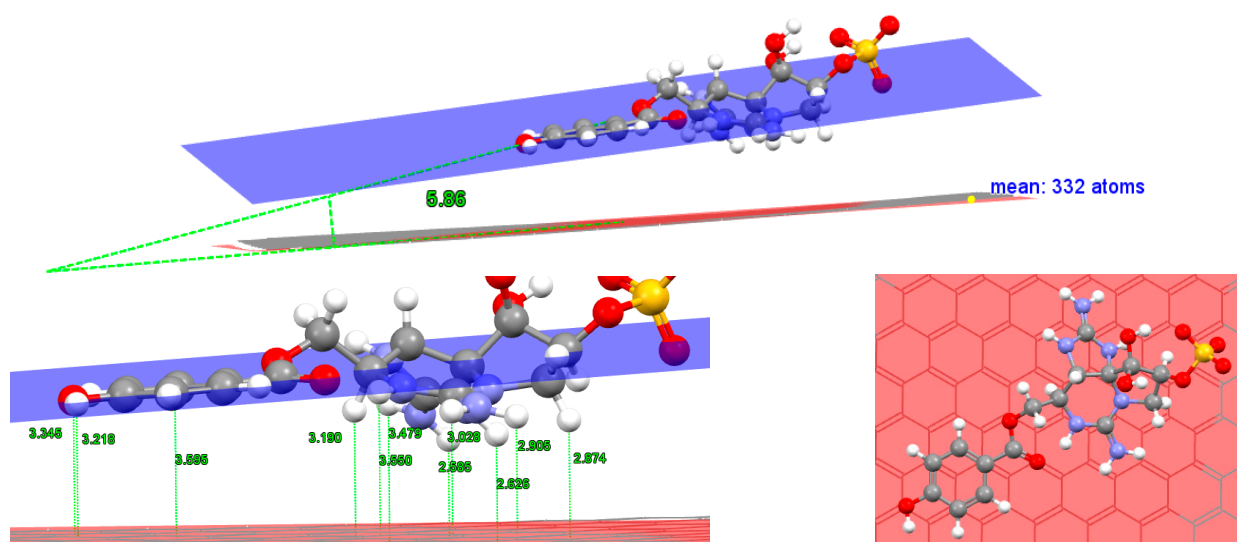


**Figure 8.** Distances for GC2's lowest energy supramolecular complex. The centroid from hydroxybenzoate carbons is located at 3.595 Å.

The supramolecular complex of GC3 has the highest energy from the N1-H series, but the energy value is close to GC2. Like GC2, we have 8 proximity contacts (Figure 9). In this case, there is no sulfate group at position 11. Therefore, the spatial distribution

of the sulfate group is directly related to the chromatographic selectivity, in this case, it favours retention.

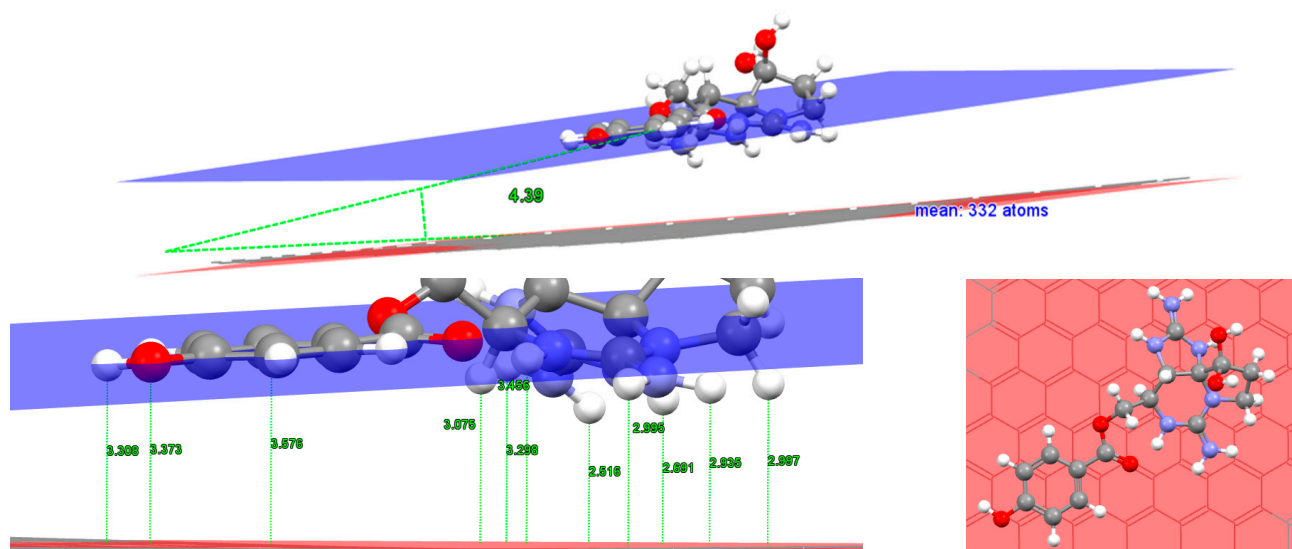


**Figure 9.** Distances for GC3's lowest energy supramolecular complex. The centroid from hydroxybenzoate carbons is located at 3.576 Å.

For all GCs, note that when graphene interacts with the non-aromatic fragment, the distance between is smaller than hydroxybenzoate (Figures 7–12). For example, the N-H guanidinium—Graphene plane is about 2.7 Å in the studied complexes, while the optimised distance in the case of the centroid for hydroxybenzoate fragment is in the range of 3.4 to 3.5 Å. The reason for this is the small atomic radius of the hydrogen atoms that come into contact with the graphene layer compared to the carbon atoms in the non-planar fragment [20].

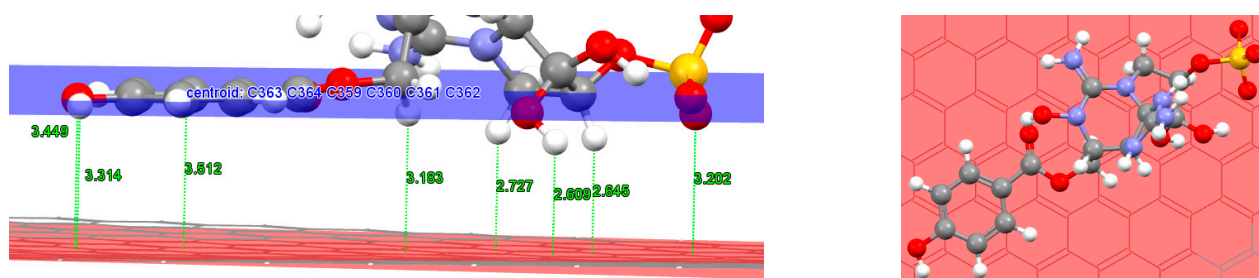


**Figure 10.** Distances for GC4's lowest energy supramolecular complex. The centroid from hydroxybenzoate carbons is located at 3.512 Å.

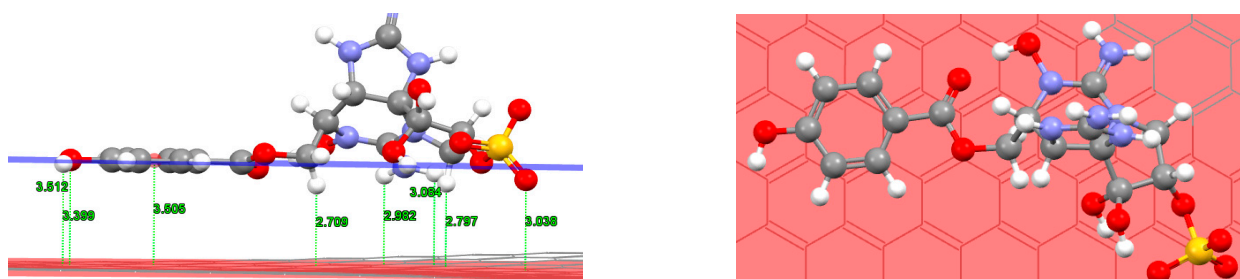


**Figure 11.** Distances for GC5's lowest energy supramolecular complex. The centroid from hydroxybenzoate carbons is located at 3.505 Å.

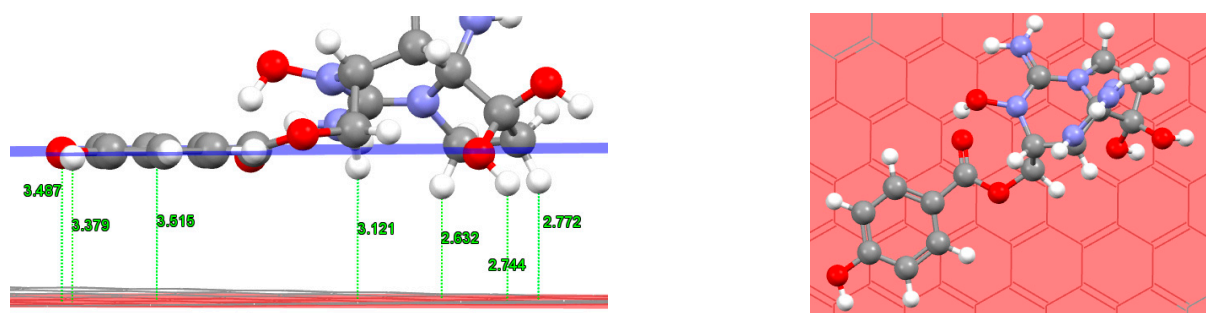


**Figure 12.** Distances for GC6's lowest energy supramolecular complex. The centroid from hydroxybenzoate carbons is located at 3.515 Å.

For GC1, GC2, and GC3, the plane angles are in the range of  $4^\circ$  to  $6^\circ$  higher than for GC4, GC5, and GC6, which are close to zero. The favourable  $\pi$ - $\pi$  interaction allows the molecules to lie flat on the surface, and the orientation of hydroxybenzoate is parallel-slipped to the graphene model. Cation- $\pi$  and hydrophobic interaction lead the molecules to form the 2D supramolecular systems. For N-H, the preferred orientation is the GC alpha-side, while for N-OH, the preferred interaction orientation is the GC delta-side.

GC4 presents only 5 close contacts. In this case, anion- $\pi$  interaction is closer than cation- $\pi$  interaction. GC5 also presents 5 close contacts, but guanidium is closer than sulfate to the graphene plane, while GC6 only presents 4 close contacts. GC6 has less favourable adsorption energy.

To evaluate the hydroxyl substituent in N1, the relative energies of GC1, GC2, and GC3 vs. GC4, GC5, and GC6 were compared. The lowest energy is found for N-H derivatives; therefore, the N1-OH group provides additional destabilization of the supramolecular interaction, either because now the lower energy orientation only faces a guanidinium group toward the graphene surface and because the alpha orientation is destabilized. For N1-H derivatives, the most preferred supramolecular complex is the orientation of positively charged guanidinium groups to the graphene surface. This interaction could be viewed as an example of a non-covalent bonding between a monopole (cation) and a quadrupole ( $\pi$  system), a Cation- $\pi$  interaction.

To gain additional insight into the  $\pi$ - $\pi$  stacking interactions, we checked the contributions to the binding energy predicted by the MMFF94 model for a series of aromatic and nonaromatic, GC4 vs dcGTX1 and GC5 vs dcGTX4, see Figure 13 for comparative purposes. Removing hydroxybenzoate from the GC4 and GC5 skeleton, less absorption energy was computed. Although the non-aromatic backbone presents more and different supramolecular close contacts, a single extrapolation of  $\pi$ - $\pi$  stacking energy could be inferred, 5–6 kcal/mol<sup>-1</sup>.

Molecular mechanic force fields are approximations of molecular behaviour, and while they can provide valuable insights, they have limitations. They are generally more accurate for smaller organic molecules and might not be as accurate for large and complex systems or specific types of non-covalent interactions. To validate our qualitative computational results, a comparison with chromatographic mimic experimental data was done.

In Figure 14, chromatographic peaks of major tentative analogues of GC molecules, commercial standards are not yet available for full assignment purposes. Chromatographic elution of GCs takes place in a clean column step, even though selective peaks can be achieved to a greater or lesser extent.

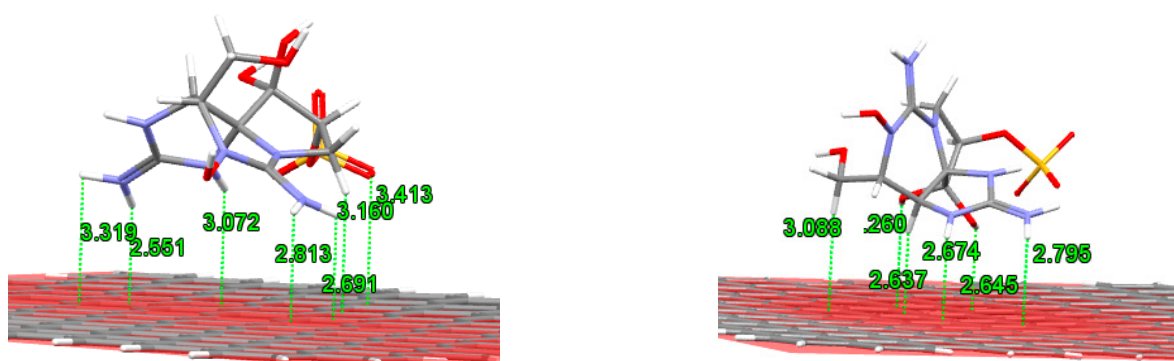


**Figure 13.** Distances for dcGTX1 (left) and dcGTX4 (right) lowest energy supramolecular complexes. Our initial MMFF94 calculations using dcGTX1 and dcGTX4 vs. GC4 and GC5 as a model binding target revealed that stacking configurations have a higher binding energy than when dicarbamoyl derivatives are approached to the graphene sheets.

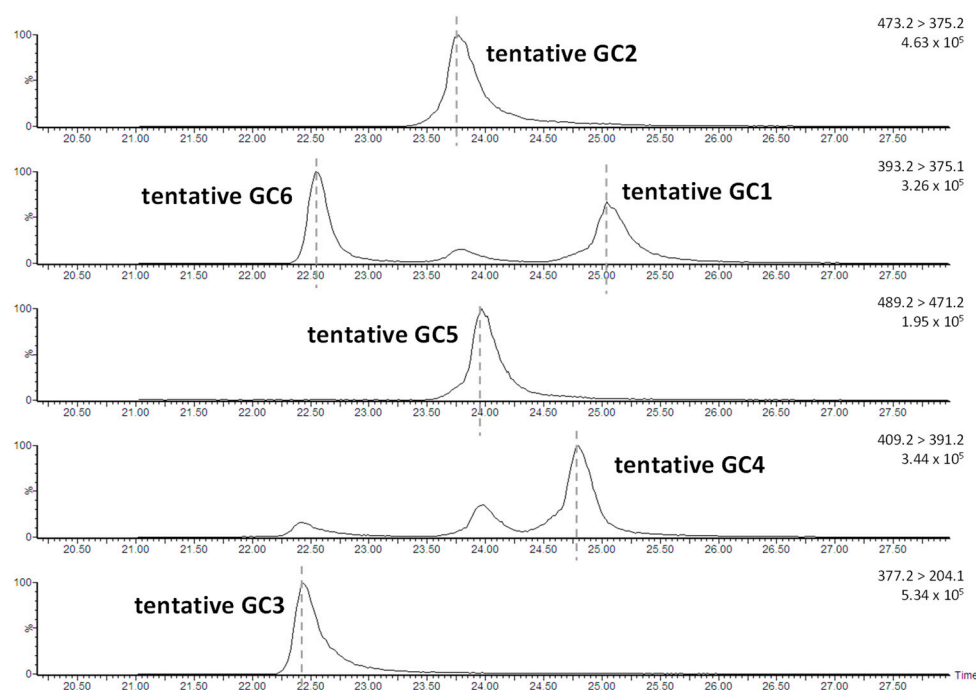


**Figure 14.** Chromatographic analysis of partially purified from large-scale cultivation of *Gymnodinium catenatum*. Six tentative main transitions were previously identified with LC-MS and chosen to be studied based on their range of retention and polarities. Tentative GC type b and other unknown toxins are also found but, in less quantity, data are not shown. Conditions: Thermo Hypercarb 3  $\mu\text{m}$ ,  $100 \times 2.1$  mm, LC column. Elution conditions; mobile phase A: water 0.1% TFA (*v/v*), mobile phase B: acetonitrile, and mobile phase C: water; gradient: 0 min [100% A]; 0.5 min [100% A]; 1.0 min [96% A, 4% B]; 8.0 min [96% A, 4% B]; 13 min [30% A, 8% B, 62% C]; 15.0 min [40% A, 13% B, 47% C]; 17.5 min [40% A, 25% B, 35% C]; 18.0 min [40% A, 40% B, 20% C]; 21.5 min [40% A, 40% B, 20% C]; 22 min [100% A]; 30 min [100% A]; flow rate: 0.25 mL/min. Temperature: 25 °C. MS detector: Waters Quattro micro using the most important MRM transitions for GCs toxins are shown. GC toxins eluted in the final stage of chromatography under re-equilibration conditions.

The experimental chromatographic elution order is from the lowest retention time, GC3-GC6-GC2-GC5-GC4-GC1, and the highest retention time. The correlation pattern of both models does not fit perfectly. However, if we consider the N1-H and N1-OH subfamilies, we can observe how the order within each of them coincides in both models,

theoretical and experimental. MMFF94 adsorption results yield qualitative agreement with experiments within N1-OH and N1-H sub-families.

Chromatographic conditions have a strong influence on the adsorption of the GCs with the stationary phase through non-binding intermolecular interactions. The percentage of acetonitrile in the mobile phase, buffer concentration, pH, and graphite surface redox state cover a full-factorial screening design for the development of elution of PSPs over the PGC platform. In our method, experimental HPLC conditions use a mixture of water and acetonitrile plus TFA as the mobile phase, and chromatographic analysis of PSTs provided the retention effect on graphite and the differentiation of analytes based on their fit to the graphite surface.

#### 4. Conclusions

Based on the experimental results and data analysis, the conclusions of the study can be summarised as follows.

1. The structure and surface polarity of graphene are promising materials for GC toxins adsorption, in the same way as in previous studies on non-aromatic PSPs analogues and tetrodotoxin and derivatives.
2. The adsorption energy values of non-aromatic were drastically decreased due to the absence of  $\pi$ - $\pi$  stacking.
3. MMFF94, like many other molecular mechanics force fields, is dependent on the initial conformation of the molecules being studied. Optimising the initial conformation is a critical step to ensure that the calculations are meaningful and accurate.
4. MMFF94 computational energy values show a qualitative correlation with the experimental elution order of GC toxins. In conclusion, an elution order prediction method was developed based on low computational cost.

**Author Contributions:** M.Á.: conceptualisation, formal analysis, investigation, supervision, writing—review and editing. M.L.: resources, supervision, funding acquisition. Á.A.: conceptualisation, methodology, formal analysis, Writing—original draft preparation. All authors have read and agreed to the published version of the manuscript.

**Funding:** This research received no external funding.

**Institutional Review Board Statement:** Not applicable.

**Informed Consent Statement:** Not applicable.

**Data Availability Statement:** The original contributions presented in the study are included in the article, further inquiries can be directed to the corresponding author/s.

**Conflicts of Interest:** The authors declare no conflicts of interest.

#### References

1. Leal, J.F.; Cristiano, M.L.S. Marine Paralytic Shellfish Toxins: Chemical Properties, Mode of Action, Newer Analogues, and Structure–Toxicity Relationship. *Nat. Prod. Rep.* **2022**, *39*, 33–57. [[CrossRef](#)] [[PubMed](#)]
2. Cifga Laboratory: Certified Reference Material Producer; CIFGA, Lugo, Spain. Available online: <https://cifga.com/> (accessed on 8 July 2023).
3. Che, Y.; Ding, L.; Qiu, J.; Ji, Y.; Li, A. Conversion and Stability of New Metabolites of Paralytic Shellfish Toxins under Different Temperature and pH Conditions. *J. Agric. Food Chem.* **2020**, *68*, 1427–1435. [[CrossRef](#)] [[PubMed](#)]
4. Duran, L.; Krock, B.; Cembella, A.; Peralta-Cruz, J.; Bustillos-Guzmán, J.J.; Band-Schmidt, C.J. Characterization of Benzoyl Saxitoxin Analogs from the Toxigenic Marine Dinoflagellate *Gymnodinium Catenatum* by Hydrophilic Interaction Liquid Ion-Chromatography-Tandem Mass Spectrometry. *Nat. Prod. Chem. Res.* **2017**, *5*, 275.
5. Negri, A.P.; Bolch, C.J.S.; Geier, S.; Green, D.H.; Park, T.-G.; Blackburn, S.I. Widespread Presence of Hydrophobic Paralytic Shellfish Toxins in *Gymnodinium Catenatum*. *Harmful Algae* **2007**, *6*, 774–780. [[CrossRef](#)]
6. Vale, P. Hydrolysis of Hydroxybenzoate Saxitoxin Analogues Originating from *Gymnodinium Catenatum*. *Food Chem.* **2011**, *125*, 1160–1165. [[CrossRef](#)]
7. Mehdi Sabzehmeidani, M.; Mahnaee, S.; Ghaedi, M.; Heidari, H.; Roy, V.A.L. Carbon Based Materials: A Review of Adsorbents for Inorganic and Organic Compounds. *Mater. Adv.* **2021**, *2*, 598–627. [[CrossRef](#)]

8. Ross, P.; Knox, J.H. *Advances in Chromatography*; Marcel Dekker, Inc.: New York, NY, USA, 1997.
9. La Tella, R.; Rigano, F.; Corman, C.; Odugbesi, G.; Donato, P.; Dugo, P.; Mondello, L. Evaluation of PGC Stationary Phases Under High-Temperature LC Conditions for the Analysis of Parabens in Food Samples. *LCGC Suppl.* **2023**, *36*, s5. [[CrossRef](#)]
10. Method Development Guide for Hypercarb Columns. Available online: <https://assets.thermofisher.com/TFS-Assets/CMD/Specification-Sheets/TG-20394-Method-Development-Guide-Hypercarb-Columns-TG20394-EN.pdf> (accessed on 8 July 2023).
11. Bhol, P.; Yadav, S.; Altaee, A.; Saxena, M.; Misra, P.K.; Samal, A.K. Graphene-Based Membranes for Water and Wastewater Treatment: A Review. *ACS Appl. Nano Mater.* **2021**, *4*, 3274–3293. [[CrossRef](#)]
12. Halgren, T.A. Merck Molecular Force Field. I. Basis, Form, Scope, Parameterization, and Performance of MMFF94. *J. Comput. Chem.* **1996**, *17*, 490–519. [[CrossRef](#)]
13. Lewis-Atwell, T.; Townsend, P.A.; Grayson, M.N. Comparisons of Different Force Fields in Conformational Analysis and Searching of Organic Molecules: A Review. *Tetrahedron* **2021**, *79*, 131865. [[CrossRef](#)]
14. Pedretti, A.; Mazzolari, A.; Gervasoni, S.; Fumagalli, L.; Vistoli, G. The VEGA Suite of Programs: An Versatile Platform for Cheminformatics and Drug Design Projects. *Bioinformatics* **2021**, *37*, 1174–1175. [[CrossRef](#)] [[PubMed](#)]
15. Antelo, Á.; Rey, V.; Álvarez, M.; Botana, A.; Botana, L. Computational Model of Adsorption for Paralytic Shellfish Poisoning Toxins (PSTs) on Graphene Surface. In Proceedings of the 20th International Electronic Conference on Synthetic Organic Chemistry session Computational Chemistry, Online, 1–31 November 2016. [[CrossRef](#)]
16. Álvarez, M.; Antelo, Á. Computational Simulation of Supramolecular Interaction Between Tetrodotoxin and Graphene. 2022. Available online: <https://sciforum.net/manuscripts/13716/manuscript.pdf> (accessed on 8 October 2023).
17. Molecules | Free Full-Text | Prediction of Chromatographic Elution Order of Analytical Mixtures Based on Quantitative Structure-Retention Relationships and Multi-Objective Optimization. Available online: <https://www.mdpi.com/1420-3049/25/13/3085> (accessed on 8 October 2023).
18. Software: Chem 3D Ultra. 18.1. Perkin Elmer. Available online: <https://www.perkinelmer.com/es/product/chemoffice-chemoffice> (accessed on 8 July 2023).
19. Software: Mercury 3.8. Available online: <http://www.Ccdc.Cam.Ac.Uk/Mercury/> (accessed on 8 July 2023).
20. Kolev, S.K.; Aleksandrov, H.A.; Atanasov, V.A.; Popov, V.N.; Milenov, T.I. Interaction of Graphene with Out-of-Plane Aromatic Hydrocarbons. *J. Phys. Chem. C* **2019**, *123*, 21448–21456. [[CrossRef](#)]

**Disclaimer/Publisher’s Note:** The statements, opinions and data contained in all publications are solely those of the individual author(s) and contributor(s) and not of MDPI and/or the editor(s). MDPI and/or the editor(s) disclaim responsibility for any injury to people or property resulting from any ideas, methods, instructions or products referred to in the content.